Large-Signal Calculations for the Overdriven Varactor Upper-Sideband Upconverter Operating at Maximum Power Output

By J. W. GEWARTOWSKI and R. H. MINETTI

(Manuscript received March 6, 1967)

When a varactor frequency upconverter is used as the output device in a communications transmitter, it is often desirable to operate at maximum power output. For such operation, the design procedure includes a large-signal analysis under overdriven conditions, requiring the use of a computer for solution.

Equations for the instantaneous varactor charge, current, and voltage are derived assuming that only three currents are present: those corresponding to the signal, pump, and output frequencies. Numerical solutions corresponding to maximum power output are obtained for both graded-junction and abrupt-junction varactors. Values of power output, conversion efficiency, input impedances, load impedance, and bias voltage are presented for ranges of drive level (1 to 2) and varactor quality ($0.001 \leqq \omega_3/\omega_c \leqq 0.1$) sufficient to include most practical designs.

I. INTRODUCTION

Varactor upconverters are finding increased application in solid-state microwave transmitters. In this application a frequency modulated IF signal is mixed with an unmodulated microwave signal to obtain a frequency modulated output signal.[1] Because of the varactor's low loss and high power handling capacity, this output signal can be used as the transmitter output signal without further amplification. Microwave conversion efficiencies in a varactor upconverter are typically greater than 50 percent.[2]

A varactor upconverter can be either an upper-sideband or a lower-sideband upconverter. However, since the lower-sideband upconverter can present stability problems,[3] the upper-sideband upconverter is generally preferred for the above application.

This paper presents a general analysis of lossy varactor upper-sideband upconverters, using both graded- and abrupt-junction varactors. Results will be presented for operation at maximum power output for a prescribed drive level. The two input signals and the output signal are all three "large" signals in this mode of operation. Penfield and Rafuse have presented a theory for nonoverdriven abrupt-junction varactors;[3] however, their analysis gives a conservative value of output power, as explained by Nelson.[4] Nelson presents an improved upper bound on the varactor charge coefficients, which results in 25 to 54 percent greater output power than that given by Penfield and Rafuse. This paper will use Nelson's method of computing this upper bound, with a slight modification to allow for arbitrary output phase angles. Grayzel has presented a similar analysis for "punch through" varactors.[5] His analysis differs from ours in that he assumes a particular phase condition for the output current [equivalent to taking $\alpha = 0$ in our (5)]. Our results show that as much as 16 percent greater power output is obtained when α is optimized.

II. ANALYSIS

2.1 *Model and Assumptions*

The varactor model chosen for the analysis is the usual one consisting of a constant resistance R_s in series with a variable capacitance, as shown in Fig. 1. A polarity is assumed such that when the varactor is reverse biased, the voltage and charge stored are positive.

For voltages between the barrier potential and the breakdown voltage, the voltage and stored charge on the variable capacitance are related by

$$\frac{v_j - \Phi}{V_B - \Phi} = \left(\frac{q - q_\Phi}{Q_B - q_\Phi}\right)^{1/(1-\gamma)} \tag{1}$$

for

$$\Phi \leqq v_j \leqq V_B$$

$$q_\Phi \leqq q \leqq Q_B ,$$

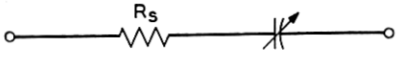

Fig. 1 — Varactor model consisting of a constant resistance in series with a time-varying capacitance.

where

v_i = voltage across the capacitance
Φ = barrier potential (negative)
V_B = breakdown voltage (positive)
q = charge on the capacitance
Q_B = charge at breakdown voltage (positive)
q_Φ = charge at the barrier potential (negative).

When the varactor is overdriven the voltage is assumed to clamp to the barrier potential

$$v_i = \Phi \quad \text{for} \quad q \leqq q_\Phi \,. \tag{2}$$

In this region the charge-storage effect is assumed to act like an infinite capacitance, so that any amount of charge can be stored without any additional voltage drop. This model is a good approximation for microwave varactors, where the minority carrier lifetime is considerably longer than an RF period. Experimental evidence has shown that this is still a reasonable approximation at frequencies as low as 40 MHz, a typical IF frequency.

It is necessary to have a parameter which measures the extent to which the varactor is overdriven. The *drive* is defined by[6]

$$drive = \frac{Q_B - q_{\min}}{Q_B - q_\Phi} \,, \tag{3}$$

where it is assumed that the varactor is always driven up to breakdown. Thus, $drive = 1$ corresponds to the "fully driven" case of Penfield and Rafuse.[3] Most practical high-power varactor devices operate overdriven, so that $drive > 1$.

Another useful parameter is the varactor cutoff frequency, given by[3]

$$f_c = \frac{\omega_c}{2\pi} = \frac{S_{\max}}{2\pi R_s} = \frac{V_B - \Phi}{2\pi R_s(1 - \gamma)(Q_B - q_\Phi)} \,, \tag{4}$$

where $S_{\max}$ is the elastance of the diode junction at the breakdown voltage. The last equivalence is obtained from (1) and the relationship $S = \partial v/\partial q$.

It will be assumed that only three currents are present in the varactor, those corresponding to the signal, pump, and output frequencies. When the pump and output frequencies are appreciably different, currents at other than the three frequencies mentioned are impeded by the selectivity characteristics of the circuits. However, if the pump and output frequencies are close together, then it is difficult to inhibit

currents at other sidebands. The effect of these sidebands on the results presented here has not been evaluated.

Circuit losses are not included explicitly. They may be accounted for by increasing the value of R_s or by calculating separate input and output circuit efficiencies, or by a combination of these two approaches.

2.2 *Equations*

The charge stored on the variable capacitance may be written as

$$q = Q_0 + 2Q_1 \sin \omega_1 t + 2Q_2 \sin \omega_2 t + 2Q_3 \sin (\omega_3 t + \alpha), \tag{5}$$

where ω_1 and ω_2 correspond to the two input frequencies, $\omega_3 = \omega_1 + \omega_2$ corresponds to the output frequency, and ω_2 is taken to be greater than ω_1. Since the two input signals at ω_1 and ω_2 are independent, their phases may be taken arbitrarily as shown. The output phase angle α, on the other hand, must be chosen to correspond to maximum power output at a prescribed value of *drive*.

The instantaneous current is obtained from (5) as

$$i = 2\omega_1 Q_1 \cos \omega_1 t + 2\omega_2 Q_2 \cos \omega_2 t + 2\omega_3 Q_3 \cos (\omega_3 t + \alpha). \tag{6}$$

The total voltage v on the varactor is given by

$$v = v_j + R_s i. \tag{7}$$

The following quantities may be obtained from (5), (6), and (7). The numerical integrations are performed using (1) and (2) for values of v_j.

Input resistance at ω_1 :

$$R_1 = R_s + \frac{1}{\omega_1 Q_1 T} \int_0^T v_j \cos \omega_1 t \, dt. \tag{8}$$

Input resistance at ω_2 :

$$R_2 = R_s + \frac{1}{\omega_2 Q_2 T} \int_0^T v_j \cos \omega_2 t \, dt. \tag{9}$$

Load resistance at ω_3 :

$$R_3 = -R_s - \frac{1}{\omega_3 Q_3 T} \int_0^T v_j \cos (\omega_3 t + \alpha) \, dt. \tag{10}$$

Input elastance at ω_1 :

$$S_1 = \frac{1}{Q_1 T} \int_0^T v_j \sin \omega_1 t \, dt. \tag{11}$$

Input elastance at ω_2 :

$$S_2 = \frac{1}{Q_2 T} \int_0^T v_i \sin \omega_2 t \, dt. \tag{12}$$

Output elastance at ω_3 :

$$S_3 = \frac{1}{Q_3 T} \int_0^T v_i \sin (\omega_3 t + \alpha) \, dt. \tag{13}$$

In general, the integration interval T must be large enough to obtain the desired degree of accuracy. To facilitate computation, ω_2 and ω_3 are selected to the nth and $(n + 1)$th integral multiples of ω_1. The integration interval is then equal to $T = 2\pi/\omega_1$. Results for nonintegrally related frequencies can be obtained from these results by interpolation.

The resistances calculated above allow one to compute the powers at the three frequencies, using values of current from (6).

Input power at ω_1 :

$$P_1 = 2\omega_1^2 Q_1^2 R_1 . \tag{14}$$

Input power at ω_2 :

$$P_2 = 2\omega_2^2 Q_2^2 R_2 . \tag{15}$$

Output power at ω_3 :

$$P_3 = 2\omega_3^2 Q_3^2 R_3 . \tag{16}$$

In most applications ω_2 and ω_3 correspond to microwave frequencies, and ω_1 corresponds to a lower frequency. Thus, we define the microwave conversion efficiency by

$$\eta_{23} = \frac{P_3}{P_2} = \frac{\omega_3^2}{\omega_2^2} \frac{Q_3^2}{Q_2^2} \frac{R_3}{R_2}. \tag{17}$$

Another useful expression for this quantity is derived in the Appendix as

$$\eta_{23} = \frac{\omega_3}{\omega_2} \frac{R_2 - R_s}{R_2} \frac{R_3}{R_3 + R_s}. \tag{18}$$

The upconversion gain is defined by

$$G_{13} = \frac{P_3}{P_1} = \frac{\omega_3^2}{\omega_1^2} \frac{Q_3^2}{Q_1^2} \frac{R_3}{R_1}. \tag{19}$$

Another useful expression for this quantity is derived in the Appendix as

$$G_{13} = \frac{\omega_3}{\omega_1} \frac{R_1 - R_s}{R_1} \frac{R_3}{R_3 + R_s}. \tag{20}$$

Equation (18) and (20) are easily seen to correspond to the results given by the Manley-Rowe[7] relations as $R_s \to 0$.

One other important parameter is the bias voltage, computed numerically from the expression

$$V_0 = \frac{1}{T} \int_0^T v_j \, dt. \tag{21}$$

2.3 *Selection of the Charge Coefficients and Output Phase Angle*

The output power P_3 as given by (16) depends on Q_3 and R_3. R_3 in turn is a function of Q_0, Q_1, Q_2, Q_3, and other parameters. These charge coefficients are selected to give maximum output power at a prescribed value of *drive*. Obviously, if the drive level were not restricted, the output power could increase without limit, since overdrive of any magnitude is allowed by the theoretical model chosen for the varactor.

The instantaneous charge is given by (5). At the onset, five independent variables are unspecified, Q_0, Q_1, Q_2, Q_3, and α. Two of these variables may be eliminated by using relationships bounding the maximum and minimum instantaneous charge. The maximum charge is given by

$$q_{\max} = Q_B \tag{22}$$

and the minimum charge is obtained from the prescribed drive level using (3). Q_B and q_Φ are, of course, known values for a given varactor.

After applying these limits to eliminate two of the variables, the remaining three variables are varied to find numerically the values corresponding to maximum output power. In our numerical process Q_0 and Q_1 are eliminated, and Q_2, Q_3, and α remain as the independent variables. Note that once these quantities are selected, all other upconverter operating parameters can be computed using the equations in Section 2.2 together with a knowledge of the varactor characteristics.

The values of $q_{\max}$ and $q_{\min}$ discussed above must be selected with some care. One method of selection would be to take maximum and minimum values directly from (5). However, this method is inclined to give different results when the frequencies are harmonically related

than when they are not. To show this, let us compare two instantaneous charge waveforms of the type of (5), both having the same charge coefficients, but the first waveform having harmonically related frequencies and the second not. The first waveform will repeat its pattern with a period $2\pi/\omega_1$, whereas the second waveform will never repeat. Evidently the second waveform will generally have a larger peak-to-peak amplitude, since it is more "random," i.e., it has a larger assortment of peaks and valleys. This is especially true when ω_2 is not much larger than ω_1.

The values of q_{max} and q_{min} are computed using Nelson's approximate method.[4] For ω_2/ω_1 greater than 2 or 3, one may visualize the ω_2 and ω_3 terms of the charge waveform as being a high-frequency signal, amplitude modulated at ω_1. Thus, one may write (5) as

$$q = Q_0 + 2Q_1 \sin \omega_1 t + R \sin (\omega_2 t + \theta), \tag{23}$$

where

$$R = 2\sqrt{Q_2^2 + Q_3^2 + 2Q_2Q_3 \cos (\omega_1 t + \alpha)}$$

$$\theta = \tan^{-1}\left[\frac{Q_3 \sin (\omega_1 t + \alpha)}{Q_2 + Q_3 \cos (\omega_1 t + \alpha)}\right].$$

Let $\omega_1 t_{max}$ and $\omega_1 t_{min}$ be the instants corresponding to the maximum and the minimum values of the functions

$$Q_1 \sin \omega_1 t \pm \sqrt{Q_2^2 + Q_3^2 + 2Q_2Q_3 \cos (\omega_1 t + \alpha)}.$$

Then, the maximum and minimum values of instantaneous stored charge are given approximately by

$$q_{max} = Q_0 + 2Q_1 \sin \omega_1 t_{max} + 2\sqrt{Q_2^2 + Q_3^2 + 2Q_2Q_3 \cos (\omega_1 t_{max} + \alpha)} \tag{24}$$

and

$$q_{min} = Q_0 + 2Q_1 \sin \omega_1 t_{min} - 2\sqrt{Q_2^2 + Q_3^2 + 2Q_2Q_3 \cos (\omega_1 t_{min} + \alpha)}. \tag{25}$$

Equations (3), (22), (24), and (25) allow one to compute Q_0 and Q_1, given the values of Q_2, Q_3, and α for a given varactor and drive level.

2.4 *Calculation Procedure*

The parameters corresponding to maximum output power were obtained from a digital computer using a computer program based upon

the simplified flow chart of Fig. 2. Trial values of α were selected at 1 degree intervals, and trial values of Q_2 and Q_3 were selected at intervals of 0.0005 ($Q_B - q_\Phi$). These values were found to give results accurate to within plotting accuracy.

III. RESULTS

As indicated in Fig. 2, the results are a function of four variables, γ, *drive*, ω_2/ω_3, and ω_3/ω_c. γ determines the varactor type, graded junction ($\gamma = \frac{1}{3}$) or abrupt junction ($\gamma = \frac{1}{2}$).

The parameter *drive* is defined by (3). There is no theoretical upper limit for this quantity for the varactor model chosen; we shall arbitrarily take 2 as the upper limit for our calculation. In a practical varactor the drive level will be limited by forward bias current due to the finite minority carrier lifetime; however, values of 2 are usually attainable.

The parameter ω_3/ω_c expresses the effect of the loss R_s for a practical varactor.

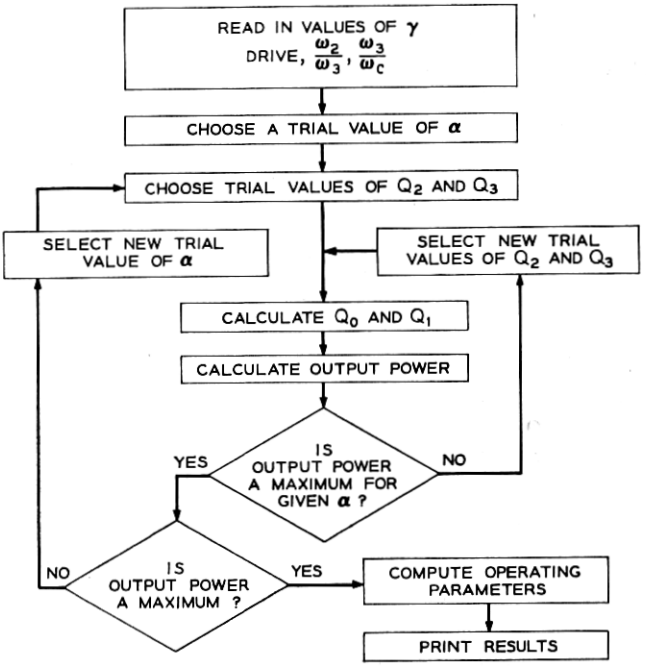

Fig. 2 — Simplified flowchart of the computer program.

The frequency ratio ω_2/ω_3 determines the ratios of the three frequencies, since $\omega_3 = \omega_1 + \omega_2$. Fortunately, it has been determined that the results can be normalized in such a way as to make them independent of this frequency ratio in most practical cases. These normalized quantities are as follows:

normalized resistances

$$\frac{R_1\omega_1}{S_{\max}}, \quad \frac{R_2\omega_2}{S_{\max}}, \quad \frac{R_3\omega_3}{S_{\max}};$$

normalized elastances

$$\frac{S_1}{S_{\max}}, \quad \frac{S_2}{S_{\max}}, \quad \frac{S_3}{S_{\max}};$$

normalized powers

$$\frac{P_1 S_{\max}}{(V_B - \Phi)^2\omega_1}, \quad \frac{P_2 S_{\max}}{(V_B - \Phi)^2\omega_2}, \quad \frac{P_3 S_{\max}}{(V_B - \Phi)^2\omega_3};$$

normalized microwave conversion efficiency and unconversion gain

$$\eta_{23}\frac{\omega_2}{\omega_3}, \quad G_{13}\frac{\omega_1}{\omega_3}; \quad \text{and}$$

normalized bias voltage

$$\frac{V_0 - \Phi}{V_B - \Phi}.$$

Results were computed for several frequency ratios. These ratios are designated by the harmonics present in the charge waveform, (5). Thus, for example, 1–7–8 denotes the case $\omega_2/\omega_1 = 7$ and $\omega_3/\omega_1 = 8$. Results were computed and compared for the cases 1–2–3, 1–3–4, 1–4–5, 1–5–6, 1–7–8, and 1–86–87. Fig. 3 shows the dependence of normalized efficiency $\eta_{23}\omega_2/\omega_3$ on the frequency ratio, for abrupt- and graded-junction varactors at the two extreme drive levels for $\omega_3/\omega_c = 0.001$. Fig. 4 shows the dependence of the normalized gain $G_{13}\omega_1/\omega_3$. Similar curves are obtained for the other operating parameters for $\omega_3/\omega_c = 0.001$. For $\omega_2/\omega_1 \geqq 5$ the percent variation in normalized resistance is less than 2 percent, and the percent variation in normalized elastance and bias voltage are less than 1 percent. As the loss factor ω_3/ω_c is increased, several of the normalized quantities show invariance as a function of the frequency ratio ω_2/ω_1 similar to that described above for $\omega_3/\omega_c = 0.001$. However, at high values of ω_3/ω_c six of these quanti-

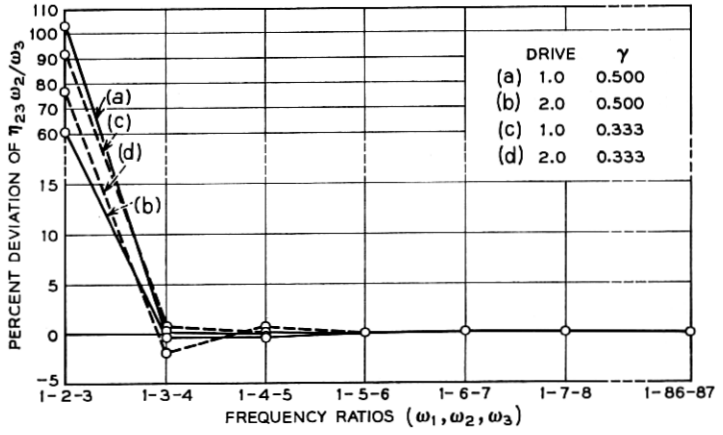

Fig. 3 — Variation of normalized microwave conversion efficiency as a function of the three upconverter frequencies. Percent deviations are calculated with respect to the 1–86–87 case. $\omega_3/\omega_c = 0.001$.

ties are no longer invariant with the ratio ω_2/ω_1. The six quantities which vary with ω_2/ω_1 are listed below (with maximum variation in percent of the 1–7–8 frequency ratio value as computed for $\omega_3/\omega_c = 0.1$):

(*i*) $R_1\omega_1/S_{max}$ (26 percent)
(*ii*) $R_2\omega_2/S_{max}$ (10 percent)
(*iii*) $P_1S_{max}/(V_B - \Phi)^2\omega_1$ (26 percent)
(*iv*) $P_2S_{max}/(V_B - \Phi)^2\omega_2$ (10 percent)
(*v*) $\eta_{23}\omega_2/\omega_3$ (9 percent)
(*vi*) $G_{13}\omega_1/\omega_3$ (35 percent).

Fortunately, simple correction functions can be applied to obtain the variation with the ratio ω_2/ω_1. Hence, all the results to be presented were computed using the 1–7–8 frequency ratios, and they may be considered to be applicable for $\omega_2/\omega_1 \geqq 5$, except for the six quantities mentioned under high-loss operation, for which simple corrections are provided.

The computed values of α for maximum power output are presented in Fig. 5. The computed values of normalized charge amplitudes for maximum power output are presented in Fig. 6 for the two extreme drive levels. As in the nonoverdriven case,[4] Q_1 and Q_2 are computed to be equal for maximum power output. Using these values and similar

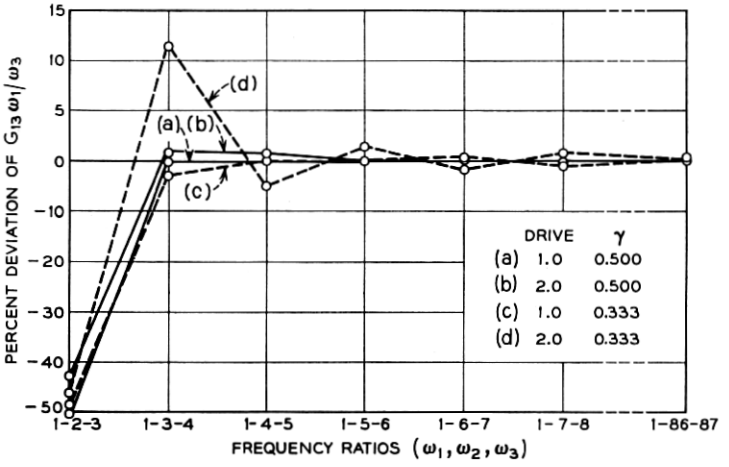

Fig. 4 — Variation of normalized upconversion gain as a function of the three upconverter frequencies. Percent deviations are calculated with respect to the 1-86-87 case. $\omega_3/\omega_c = 0.001$.

results for other drive levels, the operating characteristics of the upconverter are computed and presented below.

Figs. 7 and 8 show values of maximum output power for abrupt- and graded-junction varactors, respectively. It would appear that the abrupt-junction varactor has a considerable advantage in power output. However, if one considers the power-impedance product P_3R_3 (using data from Figs. 17 and 18), the difference is smaller; in fact, for high drive levels the graded-junction varactor has a larger P_3R_3 product.

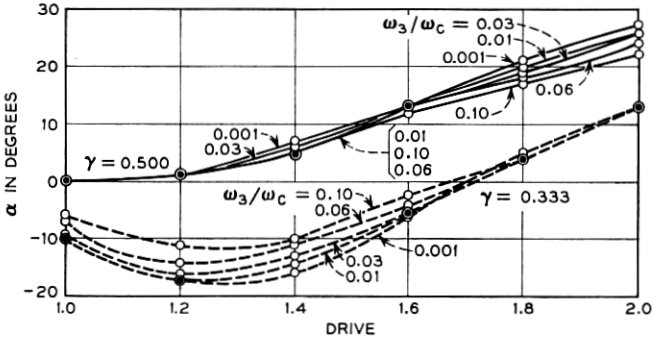

Fig. 5 — Computed values of the output current phase angle α for maximum power output.

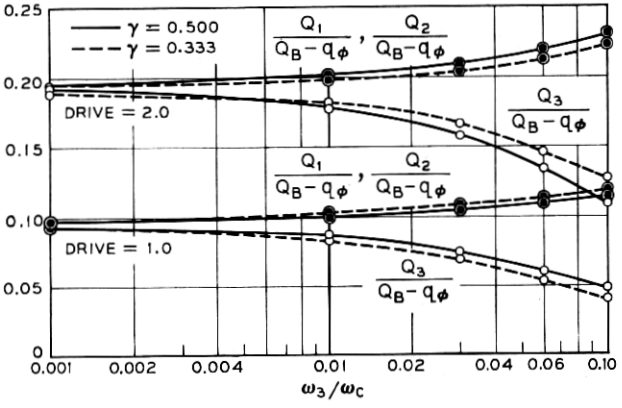

Fig. 6 — Normalized charge amplitude coefficients for maximum power output.

The results for maximum power output at unity drive agree with the results of Nelson,[4] despite the fact that Nelson assumed $\alpha = 0$ for all cases. The effect of a nonzero value of α is most pronounced for highly driven abrupt-junction varactors. For example, Fig. 7 gives a value of $P_3 S_{max}/(V_B-\Phi)^2\omega_3$ equal to 0.0327 for $\omega_3/\omega_c = 0.001$ and *drive* = 2.0, which is 16 percent larger than the value obtained assuming α equal to zero.

The upconversion gain at maximum power output is presented in Fig. 9, and the microwave conversion efficiency is plotted in Fig. 10. The correction factors for high loss and $\omega_3 \neq 8\omega_1$ are described in the

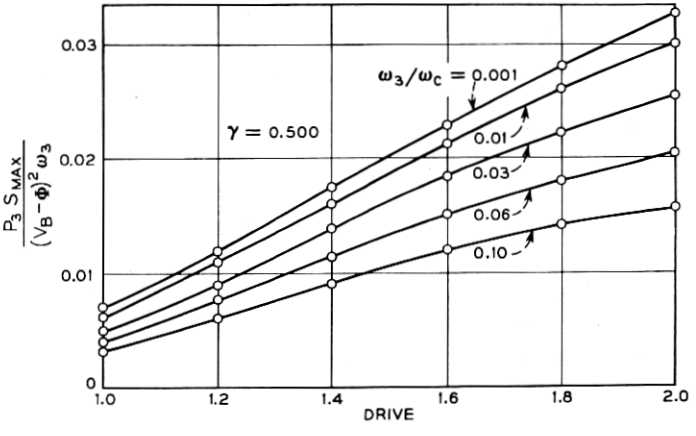

Fig. 7 — Maximum power output for abrupt-junction varactors.

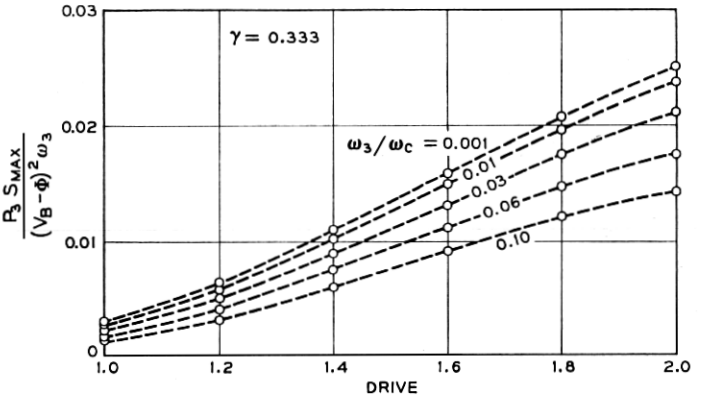

Fig. 8 — Maximum power output for graded junction varactors.

figure captions. For the graded-junction varactor, these curves show a definite advantage in operating at high drive levels. The curves are flatter for the abrupt-junction varactor and show maxima at intermediate drive levels.

Values of input elastance S_1 and S_2 are presented in Fig. 11. These

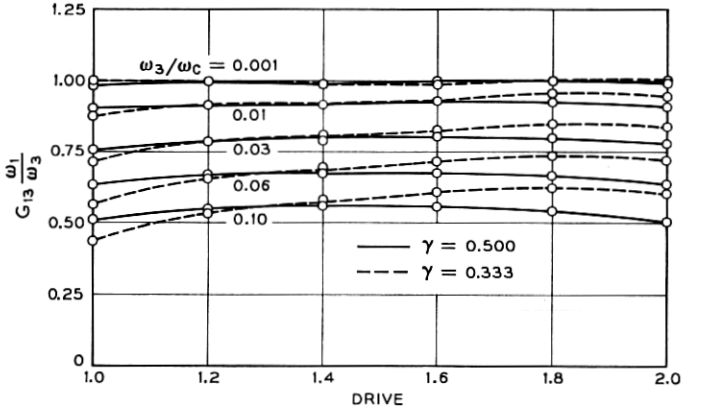

Fig. 9 — Upconversion gain for varactor upconverters operating at maximum power output. These results become inaccurate for high loss (high ω_3/ω_c) and $\omega_3 \neq 8\omega_1$. Accurate values of gain may be obtained from the values plotted by dividing by the correction factor

$$1 - \frac{\omega_3 - 8\omega_1}{8\omega_c} \frac{S_{max}}{R_1\omega_1},$$

where $R_1\omega_1/S_{max}$ is read directly from Fig. 13 or 14.

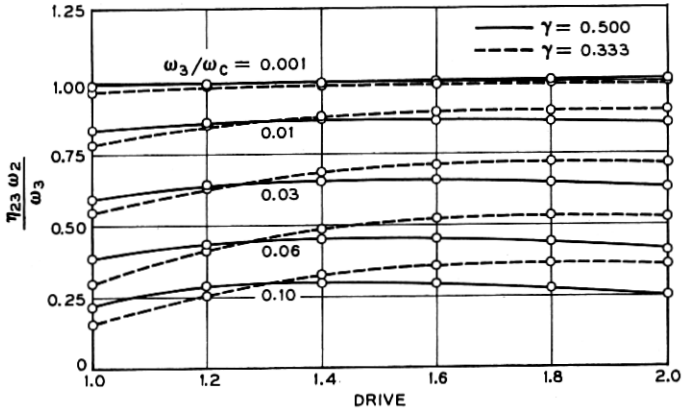

Fig. 10 — Microwave conversion efficiency for varactor upconverters operating at maximum power output. These results become inaccurate for high loss (high ω_3/ω_c) and $\omega_3 \neq 8\omega_1$. Accurate values of efficiency may be obtained from the values plotted by dividing by the correction factor

$$1 + \frac{\omega_3 - 8\omega_1}{8\omega_c}\frac{S_{max}}{R_2\omega_2},$$

where $R_2\omega_2/S_{max}$ is read directly from Fig. 15 or 16.

results are essentially independent of the loss parameter ω_3/ω_c. Values of the output elastance S_3 are presented in Fig. 12. Since S_3 was defined as the quadrature component of varactor voltage at ω_3, Kirchhoff's voltage law applied to the output loop requires that the load inductance present an equal but opposite reactance, i.e., $L_3 = S_3/\omega_3^2$.

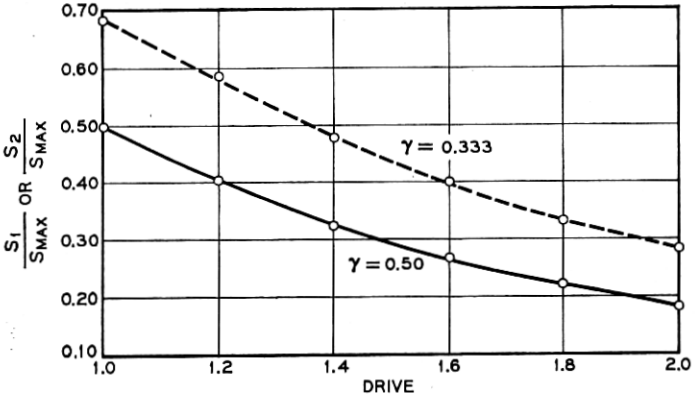

Fig. 11 — Input elastance at radian frequencies ω_1 and ω_2.

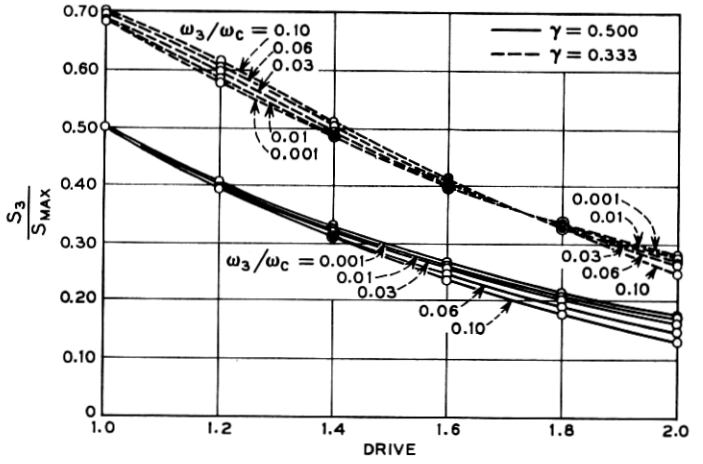

Fig. 12 — Output elastance at ω_3. The load inductance is equal to S_3/ω_3^2.

The input resistances R_1 and R_2 are presented in Figs. 13 to 16. The correction factors for high loss and $\omega_3 \neq 8\omega_1$ are described in the figure captions. The load resistance R_3 is plotted in Figs. 17 and 18. The abrupt-junction case has resistance maxima in the *drive* range of 1.4 to 1.6. This correlates with the range for maximum gain and efficiency as given by Figs. 9 and 10, as we would expect from (17) and (19). Similarly, the graded-junction case has maximum values of resistance, gain, and efficiency at a *drive* of approximately 1.8.

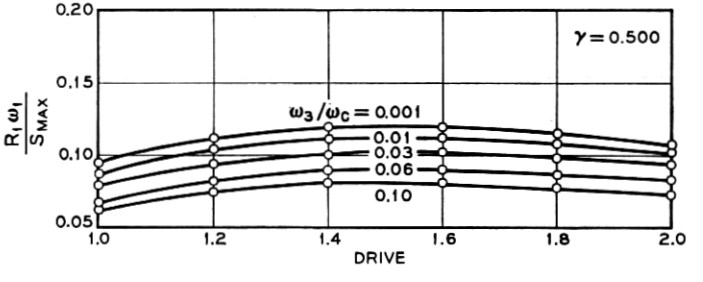

Fig. 13 — Input resistance at ω_1 for an abrupt-junction varactor. These results become inaccurate for high loss (high ω_3/ω_c) and $\omega_3 \neq 8\omega_1$. Accurate values of $R_1\omega_1/S_{max}$ may be obtained by subtracting the quantity

$$\frac{\omega_3 - 8\omega_1}{8\omega_c}$$

from the values plotted above.

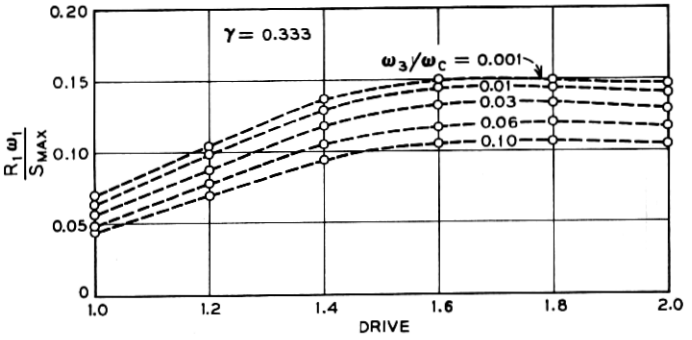

Fig. 14 — Input resistance at ω_1, for a graded-junction varactor. These results become inaccurate for high loss (high ω_3/ω_c) and $\omega_3 \neq 8\omega_1$. Accurate values of $R_1\omega_1/S_{max}$ may be obtained by subtracting the quantity

$$\frac{\omega_3 - 8\omega_1}{8\omega_c}$$

from the values plotted.

If one considers the effect of the upconverter parameters upon the instantaneous bandwidth, he finds that large bandwidth requires large values of $R_i\omega_i/S_i$. Generally, the low-frequency ω_1 circuit is most crucial in this respect. Computing ratios of $R_1\omega_1/S_1$ from Figs. 11, 13, and 14 one finds that the abrupt-junction varactor has a higher ratio

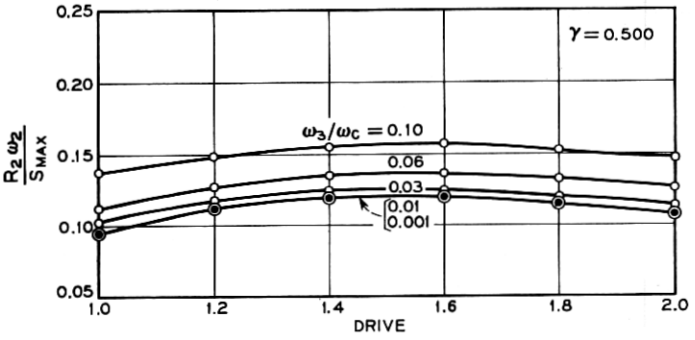

Fig. 15 — Input resistance at ω_2 for an abrupt-junction varactor. These results become inaccurate for high loss (high ω_3/ω_c) and $\omega_3 \neq 8\omega_1$. Accurate values of $R_2\omega_2/S_{max}$ may be obtained by adding the quantity

$$\frac{\omega_3 - 8\omega_1}{8\omega_c}$$

to the values plotted above.

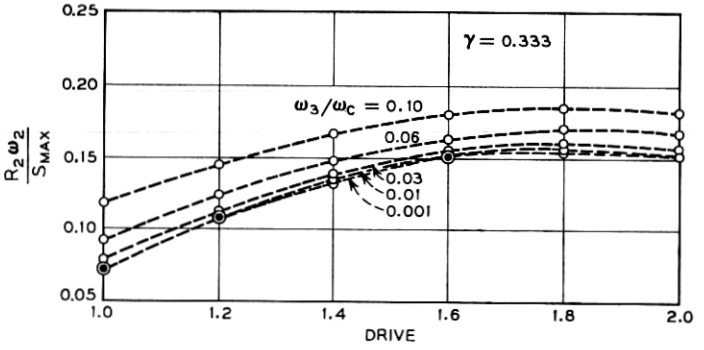

Fig. 16 — Input resistance at ω_2 for a graded-junction varactor. These results become inaccurate for high loss (high ω_3/ω_c) and $\omega_3 \neq 8\omega_1$. Accurate values of $R_2\omega_2/S_{max}$ may be obtained by adding the quantity

$$\frac{\omega_3 - 8\omega_1}{8\omega_c}$$

to the values plotted above.

at any prescribed drive level, albeit the difference becomes small (12 percent) at high drive levels. At *drive* = 1, the ratio $R_{1\omega_1}/S_1$ for the abrupt-junction varactor is nearly twice that of the graded-junction varactor.

Fig. 19 gives the dc bias voltage required for maximum output power.

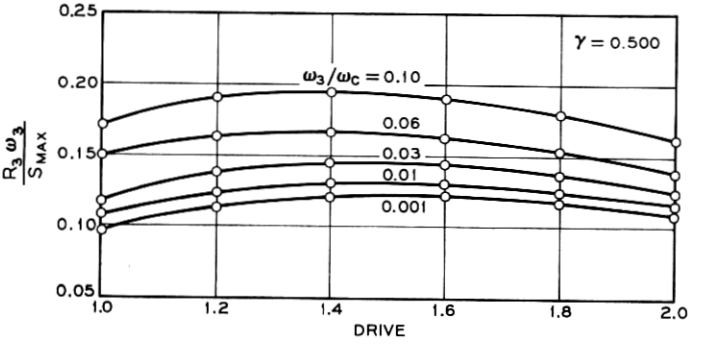

Fig. 17 — Load resistance for an abrupt-junction varactor.

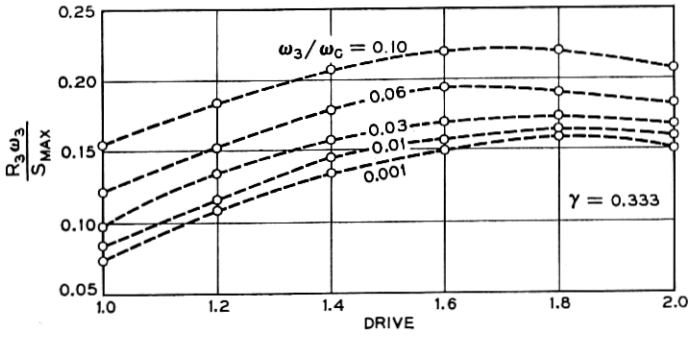

Fig. 18 — Load resistance for a graded-junction varactor.

IV. CONCLUSIONS

This analysis provides all the information required to design an upper-sideband upconverter for maximum power output, for abrupt-junction and graded-junction varactors. The results are sufficiently accurate for $\omega_2/\omega_1 \geqq 5$. The necessary load resistance and inductance are obtained from Figs. 12, 17, and 18. The input impedances at ω_1 and ω_2 are also presented, and the designer will ordinarily use this information to provide conjugate matching with the sources at these frequencies. Experimentally, the proper impedance matching conditions are facilitated by means of Swan's small-signal matching technique.[8]

It has been assumed throughout that currents are present in the varactor only at the three frequencies corresponding to the signal, pump, and upper-sideband.

At low drive levels, the abrupt-junction varactor provides both a

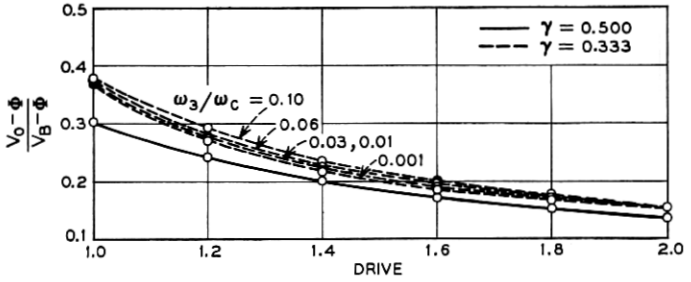

Fig. 19 — DC bias voltage required for maximum power output.

higher power-impedance product and also a greater bandwidth than that of the graded-junction varactor. However, at high drive levels the difference between the two varactor types is very small.

These results apply only to operation at maximum power output. In some applications, the designer is willing to sacrifice some power output in order to obtain a higher microwave conversion efficiency.[9] Such operation would require different operating parameters from those presented here.

APPENDIX

Efficiency and Gain Relations

The tuned upconverter may be represented by the equivalent circuit shown in Fig. 20. In this equivalent circuit the losses are separated from the frequency conversion device, and the power ratios for each are computed separately.

The power ratios for the lossless nonlinear capacitance are obtained from the Manley-Rowe relations:[7]

$$\sum_{m=0}^{\infty} \sum_{n=-\infty}^{\infty} \frac{mP'_{m+n}}{m\omega_1 + n\omega_2} = 0 \tag{26}$$

$$\sum_{m=-\infty}^{\infty} \sum_{n=0}^{\infty} \frac{nP'_{m+n}}{m\omega_1 + n\omega_2} = 0, \tag{27}$$

where P'_{m+n} is the power into the lossless nonlinear capacitance at frequency $m\omega_1 + n\omega_2$. Restricting the exchange of power to the three radian frequencies of interest ω_1, ω_2, and $\omega_3 = \omega_1 + \omega_2$, (26) gives

$$\frac{P'_1}{\omega_1} + \frac{P'_3}{\omega_3} = 0 \tag{28}$$

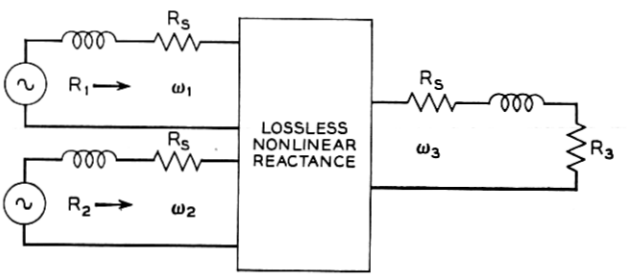

Fig. 20 — Basic equivalent circuit of the upconverter. Energy enters the nonlinear reactance at radian frequencies ω_1 and ω_2 and leaves at ω_3.

and (27) gives

$$\frac{P_2'}{\omega_2} + \frac{P_3'}{\omega_3} = 0. \tag{29}$$

In both cases P_3' is negative. If we redefine P_3' as the output power, the last two equations become

$$\frac{P_3'}{P_1'} = \frac{\omega_3}{\omega_1} \tag{30}$$

$$\frac{P_3'}{P_2'} = \frac{\omega_3}{\omega_2}. \tag{31}$$

In the input circuit at ω_2, a fraction $(R_2 - R_s)/R_2$ of the input power reaches the lossless nonlinear reactance. A fraction $R_3/(R_3+R_s)$ of the converted power reaches the load. Thus, the microwave conversion efficiency is given by

$$\begin{aligned} \eta_{23} &= \frac{R_2 - R_s}{R_2} \frac{P_3'}{P_2'} \frac{R_3}{R_3 + R_s} \\ &= \frac{\omega_3}{\omega_2} \frac{R_2 - R_s}{R_2} \frac{R_3}{R_3 + R_s}. \end{aligned} \tag{32}$$

Similarly, the upconversion gain is given by

$$G_{13} = \frac{\omega_3}{\omega_1} \frac{R_1 - R_s}{R_1} \frac{R_3}{R_3 + R_s}. \tag{33}$$

REFERENCES

1. Murphy, E. A., Posner, W., and Renkowitz, D., Solid-State 1-Watt FM Source at 6 Gc, ISSCC Digest Tech. Papers, *8*, February, 1965, pp. 104–105.
2. Hefni, I. E. and Spiwak, R. R., High-Efficiency Ultraflat Low-Noise Varactor Frequency Converter Using Low-Frequency Pumping, ISSCC Digest Tech. Papers, *9*, February, 1966, pp. 46–47.
3. Penfield, Jr., P. and Rafuse, R. P., *Varactor Applications*, MIT Press, Cambridge, Mass., 1962.
4. Nelson, C. E., A Note on the Large Signal Varactor Upper-Sideband Upconverter, Proc. IEEE, *54*. July, 1966, p. 1013.
5. Grayzel, A. I., The Design and Performance of 'Punch Through' Varactor Upper Sideband Up-Converters, NEREM Record, *8*, November, 1966, pp. 62–63.
6. Burckhardt, C. B., Analysis of Varactor Frequency Multipliers for Arbitrary Capacitance Variation and Drive Level, B.S.T.J., *44*, April, 1965, pp. 675–692.
7. Manley, J. M. and Rowe, H. E., Some General Properties of Nonlinear Elements—Part I. General Energy Relations, Proc. IRE, *44*, July, 1956, pp. 904–913.
8. Swan, C. B., Design and Evaluation of a Microwave Varactor Tripler, ISSCC Digest Tech. Papers, *8*, February. 1965, pp. 106–107.
9. Gravzel, A. I., A Note on the Abrupt Junction Large Signal Upconverter, Proc. IEEE, *54*, January, 1966, pp. 78–79.